doi:10.1016/j.jmb.2007.09.090 J. Mol. Biol. (2007) 374, 917–924

JMB

Available online at www.sciencedirect.com

ScienceDirect

ELSEVIER

COMMUNICATION

Pathways and Intermediates of Amyloid Fibril Formation

Riccardo Pellarin, Enrico Guarnera and Amedeo Caflisch*

Department of Biochemistry
University of Zürich
Winterthurerstrasse 190
CH-8057 Zürich, Switzerland

Received 18 July 2007;
received in revised form
13 September 2007;
accepted 28 September 2007
Available online
4 October 2007

The lack of understanding of amyloid fibril formation at the molecular level is a major obstacle in devising strategies to interfere with the pathologies linked to peptide or protein aggregation. In particular, little is known on the role of intermediates and fibril elongation pathways as well as their dependence on the intrinsic tendency of a polypeptide chain to self-assembly by β-sheet formation (β-aggregation propensity). Here, coarse-grained simulations of an amphipathic polypeptide show that a decrease in the β-aggregation propensity results in a larger heterogeneity of elongation pathways, despite the essentially identical structure of the final fibril. Protofibrillar intermediates that are thinner, shorter and less structured than the final fibril accumulate along some of these pathways. Moreover, the templated formation of an additional protofilament on the lateral surface of a protofibril is sometimes observed as a collective transition. Conversely, for a polypeptide model with a high β-aggregation propensity, elongation proceeds without protofibrillar intermediates. Therefore, changes in intrinsic β-aggregation propensity modulate the relative accessibility of parallel routes of aggregation.

Keywords: amyloid protofibrils; fibril growth; aggregation pathways; molecular dynamics simulations; Alzheimer's disease

Edited by F. E. Cohen

The link between protein aggregates and progressive neurodegenerative pathologies, like Alzheimer's, Parkinson's, Huntington's and prion diseases, exists but is not clear.[1,2] Despite the medical relevance of these devastating diseases, little is known about the aggregation process itself and, most importantly, how to safely inhibit the formation of toxic species. Experimental evidence indicates that early aggregates, e.g. soluble oligomers and protofibrils, have a critical role in promoting pathological effects in amyloid disorders.[3,4] As an example, the E22G mutation of the Alzheimer's peptide (Aβ) enhances protofibril formation,[5] and plaque formation is more aggressive than for wild-type Aβ in transgenic mice.[6] Also, mutations of α-synuclein that are related to early-onset forms of Parkinson's disease can produce protofibrils efficiently.[7] Yet, the molecular details and the mechanisms leading to the toxicity of these prefibrillar aggregates are only partially understood. In fact, the transient character of oligomeric precursors hinders the complete understanding of their formation process and structural details.

*Corresponding author. E-mail address: caflisch@bioc.uzh.ch.

The available experimental evidence *in vitro* indicates that the kinetics of fibril formation are complex and can be often separated into a nucleation (or lag) phase and an elongation phase,[8] followed by the equilibrium between isolated polypeptides and the fibrils.[9] Multistep kinetics with the presence of intermediates have also been reported.[10] Pathways of fibril formation, fibril morphologies and stability of protofibrillar intermediates are influenced strongly by experimental conditions (e.g. protein concentration, pH and ionic strength),[11] and elongation rates can depend on the stability of aggregation prone folding intermediates.[12]

Theoretical models have been developed to investigate the amyloid aggregation mechanism[13–15] and predict the rates[16] but strong assumptions like the irreversible association of polypeptide chains onto the fibril[13,16] are not consistent with the interpretation of experimental results.[9,17] Computer simulations using low-resolution models, which employ a simplified representation of protein geometry and energetics, have provided insights into the basic physical principles underlying protein aggregation in general,[18–20] and ordered amyloid aggregation.[21–28] However, they do not explain the wide range of aggregation processes emerging from a variety of

biophysical studies.[11,29] Atomistic models have shed some light on oligomeric aggregates and the very early steps of fibril formation,[30–36] but all-atoms simulations aimed at reproducing the kinetics and investigating the pathways of fibril formation are computationally expensive and difficult to analyze.

Earlier, we developed a phenomenological coarse-grained model of an amphipathic polypeptide and used it for exploring the kinetics of nucleation and the rates of and elongation by Langevin dynamics simulations.[37] To allow for efficient sampling, the conformational landscape of the isolated monomer was simplified such that only two states are considered: the amyloid-competent (β) and the amyloid-protected (π) states (Figure 1). In the β-state, the parallel orientation of the two intramolecular dipoles favors ordered aggregates with intermolecular dipolar interactions parallel with the fibril axis. Conversely, the π-state represents the ensemble of all polypeptide conformations that are not compatible with self-assembly into a fibril. At physiological temperature the isolated monomer undergoes a reversible isomerization from the π-state to the β-state. The energy difference between these two states can be interpreted as the β-aggregation propensity of a polypeptide sequence. For instance when $dE = E_\pi - E_\beta = 0.0$ kcal/mol, the π and β states are equally populated, whereas for $dE = -1.5$ kcal/mol and -2.5 kcal/mol the π-state is about 15 and 100 times more populated than the β state, respectively. It was found that despite the essentially identical structure of the final fibril, ordered aggregation of a polypeptide with a stable β-state follows a pathway devoid of stable intermediates, while on-pathway micellar oligomers (with hydrophilic surface and hydrophobic interior) were observed during the nucleation phase of a polypeptide with a β-state that is marginally stable. In other words, high and low β-prone sequences show significantly different nucleation processes. These two models are termed β-stable and β-unstable, respectively, and the passage from one regime to the other was achieved by varying solely the parameter dE.[37] The focus of our previous study was on the nucleation phase, while the elongation mechanism and pathway(s) were not investigated. Here, for each of four

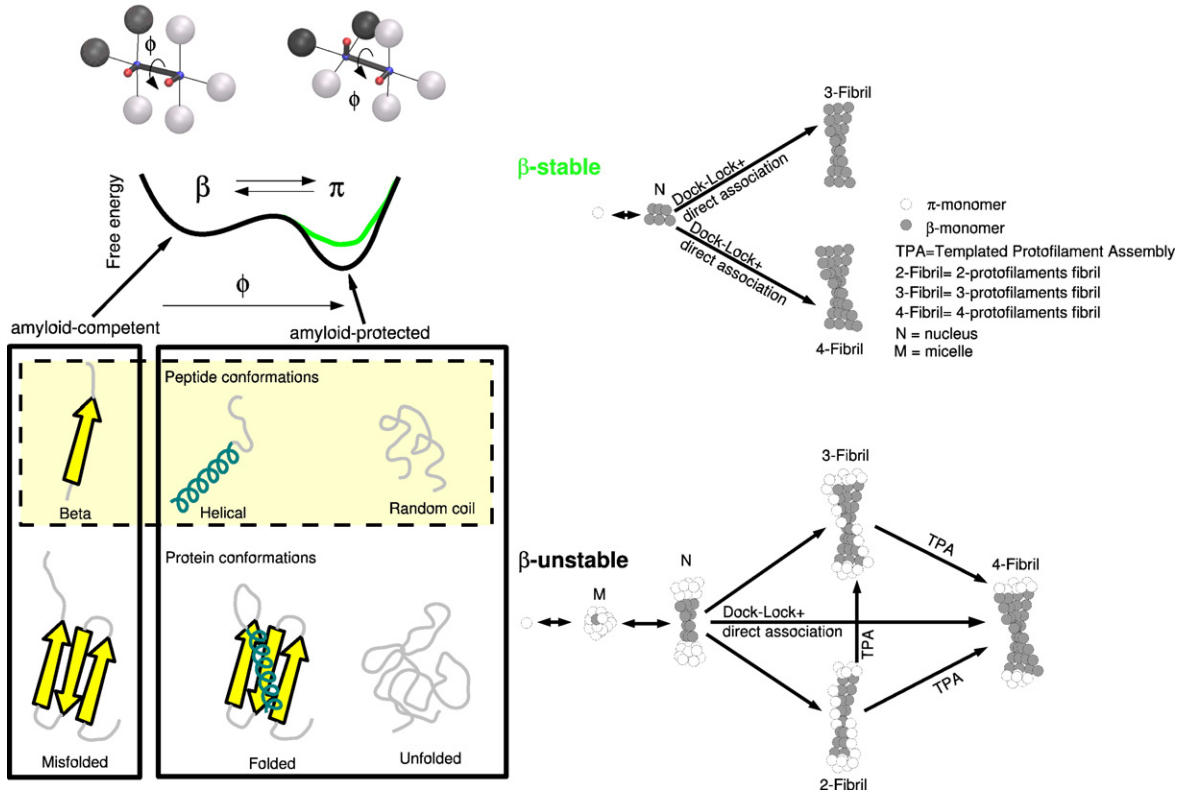

Figure 1. The model and aggregation pathways. Left: Sticks and beads representations of the monomer in the amyloid-competent state β and the amyloid-protected state π. The large spheres are hydrophobic (black) and hydrophilic (gray), while the two dipoles are shown with small red and blue spheres. The β and π states of the monomer are shown on top of the two corresponding minima of the free energy, plotted as a function of the dihedral angle ϕ of the two dipoles. Note that the population of monomers in the β-state decreases by lowering the free energy of the π-state, as indicated by the green and black profiles. For each value of the β-aggregation propensity dE ($dE = E_\pi - E_\beta = -1.5$, -2.0, -2.25, -2.5 kcal/mol) 100 Langevin dynamics runs with different initial assignments of the velocities were started from 125 monomers uniformly distributed in a box with random orientations. All simulations were carried out at a temperature of 310 K and a concentration of 8.5 mM with the same force-field parameters as those used previously.[37] Results discussed in this work refer mainly to the β-stable ($dE = -1.5$ kcal/mol) and the β-unstable ($dE = -2.5$ kcal/mol) models. Right: Observed aggregation pathways for the β-stable and β-unstable models. The elongation pathways of the latter are more heterogeneous than those of the former.

polypeptide models (four values of dE that range from β-stable to β-unstable) 100 Langevin dynamics runs were performed to explore the elongation phase; i.e. the pathway(s) leading from the nucleus to the final fibril.

The present work was motivated by the following two questions: what is the influence of the intrinsic β-aggregation propensity on the mechanism of fibril elongation? and are there multiple pathways and/or intermediates? From a detailed analysis of the simulations (started from 125 coarse-grained monomers in a monodisperse state), a rich scenario of alternative pathways, some with prefibrillar intermediates, emerges only for monomers with a low β-aggregation propensity. The simulation results go beyond the fibril formation mechanisms suggested on the basis of biophysical measurements, and have strong implications for the design of inhibitors of amyloid aggregation.

Terminology

A rigorous terminology for the early aggregates and intermediates of amyloid self-assembly observed *in vitro* has been recently summarized.[38,39] Because the computer simulations allow for the detailed investigation of individual oligomers as well as prefibrillar states and the final fibril, it is useful and straightforward to define the following nomenclature: a protofilament is a file of monomers with intermolecular dipolar interactions parallel with its axis; a protofibril is a transient structure that consists of two to three protofilaments with large unstructured regions; and the final fibril is a fully ordered aggregate of three to four protofilaments. In the model used here, the fibril is stabilized by intermolecular dipolar interactions within each protofilament and van der Waals interactions between hydrophobic beads.[37]

Aggregation state network

An aggregate consists of monomers whose mutual minimal distances are less than 6 Å, and it is isolated using a clustering procedure as described.[37] Three progress variables are used to monitor the aggregation process: the size of the largest aggregate N_{la}, the number of monomers in the β-state within the largest aggregate N_{la}^{β}, and the number of protofilaments in the largest aggregate N_{la}^{pf}. Note that the range of N_{la} is limited by the size of the simulated system ($1 \leq N_{la} \leq 125$). The number of protofilaments within a single aggregate is calculated by counting the files of monomers in the β-state with intermolecular dipolar interactions. Let N_f be the number of such files present into a given aggregate, and $\omega_1, \cdots, \omega_{Nf}$ the number of monomers in each file (with $\omega_i > 10$ to reduce noise). The number of protofilaments in aggregate a, N_a^{pf}, is thus defined as:

$$N_a^{pf} = \frac{\left(\sum_{i=1}^{N_f} \omega_i\right)^2}{\sum_{i=1}^{N_f} \omega_i^2} \qquad (1)$$

This definition prevents counting small isolated files whose formation is a result of thermal fluctuations, enhancing the signal to noise ratio with respect to N_f. Two limiting cases are useful to explain this variable. In the case that all files have the same size (i.e. $\omega_1 = \ldots = \omega_{Nf}$), the protofilament number N_a^{pf} is equal to the number of files N_f. In the case where a single ω_i predominates ($\omega_i \gg \omega_k$ for all k different from i) N_a^{pf} tends to 1. The number of protofilaments in the largest aggregate N_{la}^{pf} is thus the function N_a^{pf} applied to the largest of all aggregates present in the simulation volume. Selected time series of N_{la}, N_{la}^{β} and N_{la}^{pf} are reported in Figure 2.

The aggregation state network (Figure 3) is a graph in which states and direct transitions observed during the Langevin dynamics simulations are displayed as nodes and links, respectively.[40] Furthermore, the size of each node reflects the statistical weight of the corresponding state. In this way, metastable states and their dynamic connectivity are illustrated without requiring projections onto arbitrarily chosen reaction coordinates.[41] Micellar oligomers (white nodes, $N_{la} \sim 20, N_{la}^{pf} = 0$), which are spherical aggregates whose core consists of the hydrophobic spheres of the monomers (see inset A of Figure 3),[37] and fibrils (red nodes, $N_{la} \sim 100$, $N_{la}^{pf} = 4$) are the most populated states during the lag phase and the final equilibrium, respectively. Strikingly, a greater variety of aggregation mechanisms emerges for the β-unstable (Figure 3, bottom) than the β-stable polypeptide model (Figure 3, top). In particular, the former shows the presence of intermediates, i.e. protofibrils consisting of only two (green nodes) or three (blue nodes) protofilaments. Moreover, the aggregation state network qualitatively illustrates that the protofibrils are metastable and it displays broad transition regions between the two-protofilament state and the three-protofilament state, as well as between the latter and the final fibril.

Templated protofilament assembly

Previously, the elongation rate was found to increase according to the population of the amyloid-competent state,[37] but the underlying mechanism of elongation was not investigated. Using the Markov chain formalism (see the Supplementary Data) it is possible to estimate the rate of association of a monomer to a fibril followed by the isomerization from the amyloid-protected state to the amyloid-competent state (k_{fibril}). An alternative process is the monomer isomerization in the solvent followed by association ($k_{solvent}$). In their analytical model of fibril elongation, Massi and Straub have illustrated these two pathways as the route of monomer association to the fibril followed by isomerization (deposition and reorganization in Figure 4 of Massi & Straub[14]) and the route of direct association (direct deposition in Figure 5 of Massi & Straub[14]). The former pathway corresponds to the dock-lock mechanism.[42–44] Hence, the ratio $k_{fibril}/k_{solvent}$ measures the efficiency of the dock-lock mechanism; it is

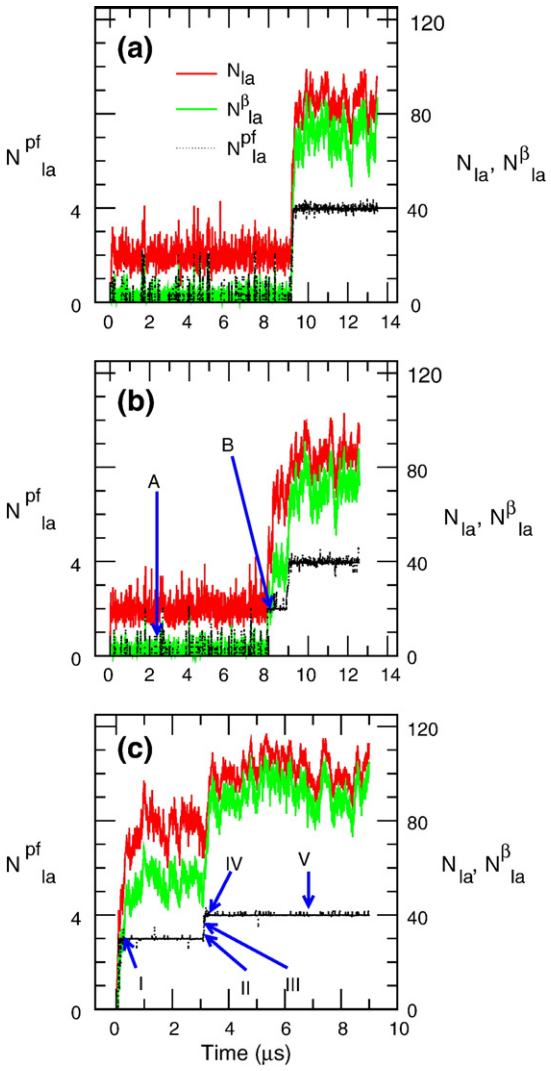

Figure 2. Protofibrillar intermediates and pathway heterogeneity. The time-series of three progress variables are used to monitor the evolution of the largest aggregate (1a) in the β-unstable simulations: The number of protofilaments N_{la}^{pf} (black curve with the *y*-axis description on the left; note that this quantity is evaluated by equation (1) and can be non-integer), the size of the largest aggregate N_{la} and the number of monomers in β-state N_{la}^{β} (red and green curves, respectively, with the *y*-axis description on the right). The three runs shown are representative of (a) elongation without intermediates, and (b) with two-filament or (c) three-filament protofibrillar intermediates. Templated protofilament assembly is observed at about 9 μs in (b) and at about 3 μs in (c), and the snapshots labeled are shown in Figure 3.

3.6 for the β-unstable model and 6.6 for the β-stable model. In both cases, the rate of conversion of a monomer bound to a fibril exceeds that in solution, suggesting that the elongation is dominated by a dock-lock mechanism. Nevertheless, this mechanism does not exclude collective conversions.

Representative time series of the number of protofilaments N_{la}^{pf} are shown by a black curve in Figure 2 for the β-unstable model. Metastable intermediates are observed in about half of the runs (see Supplementary Data). Interestingly, during some of the fast transitions from a three-protofilament aggregate to the final fibril (or sporadically from two to three-protofilament protofibrils) the size of the largest aggregate (red line) does not change significantly, whereas its number of monomers in the β-state (green line) increases abruptly, e.g. at about 9 μs and 3 μs in Figure 2(b) and (c), respectively. The collective conversion of monomers from the amyloid-protected to the amyloid-competent state is a consequence of the templated assembly of the fourth filament on the metastable protofibril consisting of three protofilaments (Figure 3 insets I–V). In other words, a file of monomers in the amyloid-protected conformation accumulates, first without forming intermolecular dipolar interactions, along the exposed hydrophobic surface of the three-protofilament aggregate (blue monomers in inset I). This event is then followed by a collective transition during which all monomers in the file convert to the β-state, which is stabilized by both intermolecular dipole interactions within the fourth protofilament and van der Waals interactions with monomers in the other three protofilaments (insets II–IV). The templated-assembly mechanism observed in the simulations is consistent with measurements of insulin aggregation by atomic force microscopy.[45] Moreover, protofibril maturation into fibrils is irreversible under the conditions used in the present simulations, i.e. 310 K and 8.5 mM (see Figure 2). Irreversibility has been suggested on the basis of the temporal increase in average protofibril size measured by quasi-elastic light-scattering spectroscopy.[46]

Analysis of the time series of the β-stable model does not reveal any event of templated protofilament formation. In fact, fibrils composed of three protofilaments contain as many monomers in the β-state as the mature four-protofilament fibril (see Figure 4(d)); thus, the formation of the fourth protofilament corresponds to a redistribution of monomers in the β-state among the protofilaments.

Size and structural characterization of protofibrils

The size distribution of the two and three-protofilament aggregates are different and depend on the β-aggregation propensity of the monomer (Figure 4). During the elongation phase, intermediates with two protofilaments are observed mainly for the β-unstable model (peak at $N_{la} \sim 70$). By raising the β-aggregation propensity (from $dE = -2.5$ kcal/mol to $dE = -1.5$ kcal/mol) there is a decrease in the average aggregation size of two-protofilament aggregates. Protofibrils consisting of three protofilaments are observed during the elongation phase of all models. Notably, by increasing the β-aggregation tendency, the number of runs with on-pathway intermediates decreases monotonically, which reflects the lower heterogeneity of pathways for the β-stable model.

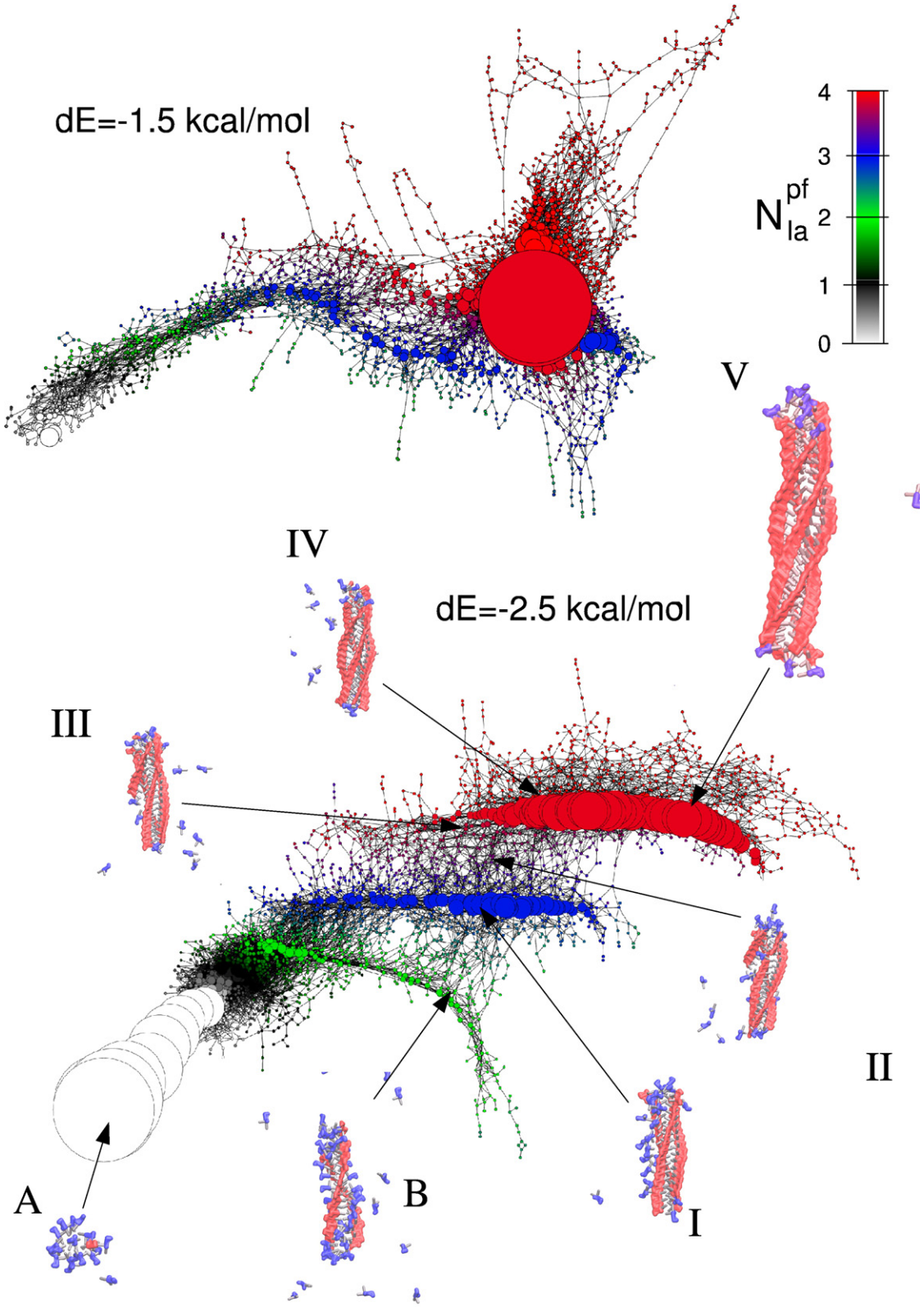

Figure 3. Aggregation state network. The size of the largest aggregate N_{la} and its number of protofilaments N_{la}^{pf} were used to cluster all snapshots into states (i.e. nodes of the network). The size and color of the nodes correspond to the statistical weight and the number of protofilaments N_{la}^{pf}, respectively. Links are direct transitions within 0.5 ns (10,000 steps of 50 fs each) of Langevin dynamics. All the states and the transitions that have been explored by the simulations are represented in these networks. Note the much higher heterogeneity of protofibrillar intermediates for the β-unstable ($dE = -2.5$ kcal/mol, bottom) than the β-stable ($dE = -1.5$ kcal/mol, top) model. The insets show the structures of the largest aggregates from the snapshots labeled in Figure 2. In these structures, monomers in the amyloid-competent conformer β and amyloid-protected conformer π are in red and blue, respectively. Furthermore, hydrophobic spheres are gray and hydrophilic spheres are not shown for visual clarity.

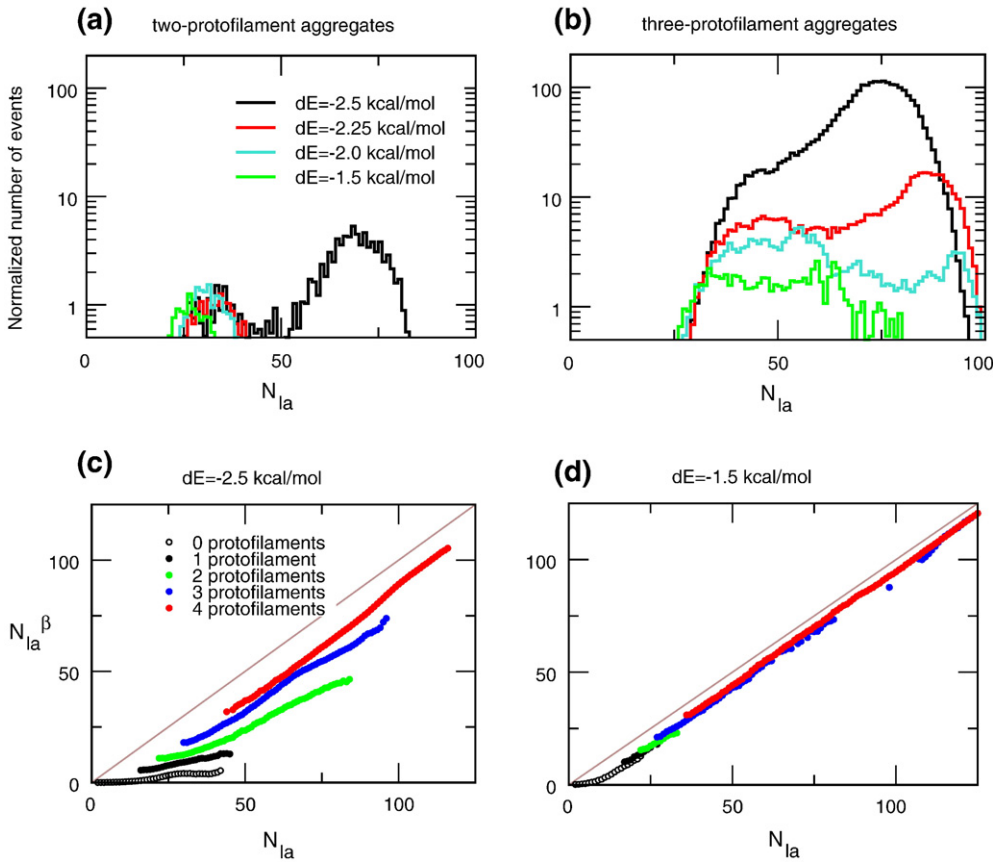

Figure 4. Size distribution of (a) two-protofilament and (b) three-protofilament protofibrils during fibril growth. The histograms are built by counting the trajectory frames in which the largest aggregate contains either two or three protofilaments. The frames are collected only during the elongation phase, i.e. after the nucleation step and before reaching the final monomer/fibril equilibrium. Average value of the number of monomers in β-state contained into the largest aggregate, as a function of the size of the largest aggregate for the (c) β-unstable and (d) the β-stable models.

For the β-unstable model protofibrils are thinner, shorter and more disordered than the final fibril. The protofibrils and fibrils of this model often present deposits of monomers in the π-state that are not involved in intermolecular dipole interactions and are highly disordered (blue monomers in the insets of Figure 3). The ratio between the number of monomers in the β-state and the total number of monomers N_{la}^{β}/N_{la} is significantly smaller than 1, even for fibrils consisting of four protofilaments (Figure 4(c)). The deviation is due mainly to the fibril ends that are populated by monomers in the π-state (see Figure 3 inset V). Furthermore, protofibrils with two or three protofilaments contain less monomers in the β-state than the four-protofilament fibril of the same size. Conversely, for the β-stable model the N_{la}^{β}/N_{la} ratio is always close to 1, and aggregates of three protofilaments can have more than 100 monomers (Figure 4(d)).

Conclusions

The self-assembly process of an amphipathic polypeptide has been investigated by multiple Langevin dynamics simulations using a coarse-grained model whose simplicity allows for the sampling of hundreds of fibril formation events. By varying a single parameter of the model, namely the relative stability of the amyloid-competent and amyloid-protected states of the polypeptide (β-aggregation propensity), interesting insights into elongation pathways and protofibrillar intermediates have been obtained. Two main observations emerge from the simulation results.

First, the roughness of the free-energy surface governing the aggregation process and the heterogeneity of pathways of fibril elongation increase by reducing the β-aggregation propensity. Hence, a mutation that decreases the β-aggregation tendency could result in greater variety of prefibrillar aggregates. Interestingly, these simulation results provide a possible explanation for the enhanced *in vitro* formation of oligomers and protofibrils of the Arctic mutant (E22G) of the Alzheimer's Aβ peptide,[5] and the A30P mutant of α-synuclein.[7] In fact, among the 20 standard amino acids, glycine and proline residues have the weakest propensity of β-sheet formation,[47] and β-aggregation.[48]

Second, a mechanism of templated protofilament assembly is sometimes observed during fibril growth. Although the elongation is accomplished mainly by dock-lock monomer addition at the

growing ends, the formation of an ordered protofilament can occur at the lateral surface of a protofibril by collective interconversion of a file of previously deposited monomers. This mechanism is particularly frequent for the model with low β-aggregation propensity, where, due to the frustration of the conformational landscape, the isomerization of a single monomer is strongly disfavored.

In conclusion, the simulation results provide strong evidence of multiple routes of polypeptide self-assembly. Notably, a reduction of the intrinsic β-aggregation propensity induces higher pathway heterogeneity and on-pathway protofibrillar intermediates. Given the experimental evidence of toxicity of prefibrillar aggregates, one is tempted to speculate that therapeutic strategies aimed at reducing fibril-formation propensity (e.g. stabilization of the folded state by small molecules) might paradoxically promote the accumulation of toxic species.

Acknowledgements

We thank F. Marchand and M. Convertino for interesting discussions, and S. Muff for comments on the manuscript. The simulations were performed on the Matterhorn cluster of the University of Zurich, and we gratefully acknowledge the support of C. Bolliger and A. Godknecht. This work was supported by a Swiss National Science Foundation grant and the National Competence Center for Research (NCCR) in Neural Plasticity and Repair.

Supplementary Data

Supplementary data associated with this article can be found, in the online version, at doi:10.1016/j.jmb.2007.09.090

References

1. Dobson, C. M. (2003). Protein folding and misfolding. *Nature*, **426**, 884–890.
2. Lansbury, P. T. & Lashuel, H. A. (2006). A century-old debate on protein aggregation and neurodegeneration enters the clinic. *Nature*, **443**, 774–779.
3. Haass, C. & Selkoe, D. J. (2007). Soluble protein oligomers in neurodegeneration: lessons from the Alzheimer's amyloid β-peptide. *Nature Rev. Mol. Cell Biol.* **8**, 101–112.
4. Caughey, B. & Lansbury, P. T. (2003). Protofibrils, pores, fibrils, and neurodegeneration: separating the responsible protein aggregates from the innocent bystanders. *Annu. Rev. Neurosci.* **26**, 267–298.
5. Nilsberth, C., Westlind-Danielsson, A., Eckman, C. B., Condron, M. M., Axelman, K., Forsell, C. *et al.* (2001). The 'Arctic' APP mutation (E693G) causes Alzheimer's disease by enhanced Abeta protofibril formation. *Nature Neurosci.* **4**, 887–893.
6. Cheng, I. H., Palop, J. J., Esposito, L. A., Bien-Ly, N., Yan, F. & Mucke, L. (2004). Aggressive amyloidosis in mice expressing human amyloid peptides with the Arctic mutation. *Nature Med.* **10**, 1190–1192.
7. Conway, K. A., Lee, S. J., Rochet, J. C., Ding, T. T., Williamson, R. E. & Lansbury, P. T. (2000). Acceleration of oligomerization, not fibrillization, is a shared property of both alpha-synuclein mutations linked to early-onset Parkinson's disease: implications for pathogenesis and therapy. *Proc. Natl Acad. Sci. USA*, **97**, 571–576.
8. Lomakin, A., Chung, D. S., Benedek, G. B., Kirschner, D. A. & Teplow, D. B. (1996). On the nucleation and growth of amyloid β-protein fibrils: detection of nuclei and quantitation of rate constants. *Proc. Natl Acad. Sci. USA*, **93**, 1125–1129.
9. O'Nuallain, B., Shivaprasad, S., Kheterpal, I. & Wetzel, R. (2005). Thermodynamics of Aβ(1-40) amyloid fibril elongation. *Biochemistry*, **44**, 12709–12718.
10. Kelly, J. W. (1998). The alternative conformations of amyloidogenic proteins and their multi-step assembly pathways. *Curr. Opin. Struct. Biol.* **8**, 101–106.
11. Gosal, W. S., Morten, I. J., Hewitt, E. W., Smith, D. A., Thomson, N. H. & Radford, S. E. (2005). Competing pathways determine fibril morphology in the self-assembly of β2-microglobulin into amyloid. *J. Mol. Biol.* **351**, 850–864.
12. Jahn, T. R., Parker, M. J., Homans, S. W. & Radford, S. E. (2006). Amyloid formation under physiological conditions proceeds *via* a native-like folding intermediate. *Nature Struct. Mol. Biol.* **13**, 195–201.
13. Lomakin, A., Teplow, D. B., Kirschner, D. A. & Benedek, G. (1997). Kinetic theory of fibrillogenesis of amyloid β-protein. *Proc. Natl Acad. Sci. USA*, **94**, 7942–7947.
14. Massi, F. & Straub, J. E. (2001). Energy landscape theory for Alzheimer's amyloid β-peptide fibril elongation. *Proteins: Struct. Funct. Bioinformatics*, **42**, 217–229.
15. Modler, A. J., Gast, K., Lutsch, G. & Damaschun, G. (2003). Assembly of amyloid protofibrils *via* critical oligomers–a novel pathway of amyloid formation. *J. Mol. Biol.* **325**, 135–148.
16. Hall, D., Hirota, N. & Dobson, C. M. (2005). A toy model for predicting the rate of amyloid formation from unfolded protein. *J. Mol. Biol.* **351**, 195–205.
17. Carulla, N., Caddy, G. L., Hall, D. R., Zurdo, J., Gairi, M., Feliz, M. *et al.* (2005). Molecular recycling within amyloid fibrils. *Nature*, **436**, 554–558.
18. Broglia, R. A., Tiana, G., Pasquali, S., Roman, H. E. & Vigezzi, E. (1998). Folding and aggregation of designed proteins. *Proc. Natl Acad. Sci. USA*, **95**, 12930–12933.
19. Gupta, P., Hall, C. K. & Voegler, A. C. (1998). Effect of denaturant and protein concentrations upon protein refolding and aggregation: a simple lattice model. *Protein Sci.* **7**, 2642–2652.
20. Harrison, P. M., Chan, H. S., Prusiner, S. B. & Cohen, F. E. (1999). Thermodynamics of model prions and its implications for the problem of prion protein folding. *J. Mol. Biol.* **286**, 593–606.
21. Dima, R. I. & Thirumalai, D. (2002). Exploring protein aggregation and self-propagation using lattice models: phase diagram and kinetics. *Protein Sci.* **11**, 1036–1049.
22. Urbanc, B., Cruz, L., Yun, S., Buldyrev, S. V., Bitan, G., Teplow, D. B. & Stanley, H. E. (2004). In silico study of amyloid β-protein folding and oligomerization. *Proc. Natl Acad. Sci. USA*, **101**, 17345–17350.
23. Nguyen, H. D. & Hall, C. K. (2004). Molecular

dynamics simulations of spontaneous fibril formation by random-coil peptides. *Proc. Natl Acad. Sci. USA*, **101**, 16180–16185.
24. Jang, H., Hall, C. K. & Zhou, Y. (2004). Assembly and kinetic folding pathways of a tetrameric beta-sheet complex: molecular dynamics simulations on simplified off-lattice protein models. *Biophys. J.* **86**, 31–49.
25. Khare, S. D., Ding, F., Gwanmesia, K. N. & Dokholyan, N. V. (2005). Molecular origin of polyglutamine aggregation in neurodegenerative diseases. *PLoS Comput. Biol.* **1**, 230–235.
26. Chen, Y. & Dokholyan, N. V. (2005). A single disulfide bond differentiates aggregation pathways of beta2-microglobulin. *J. Mol. Biol.* **354**, 473–482.
27. Malolepsza, E., Boniecki, M., Kolinski, A. & Piela, L. (2005). Theoretical model of prion propagation: a misfolded protein induces misfolding. *Proc. Natl Acad. Sci. USA*, **102**, 7835–7840.
28. Bellesia, G. & Shea, J.-E. (2007). Self-assembly of beta-sheet forming peptides into chiral fibrillar clusters. *J. Chem. Phys.* **126**, 245104.
29. Plakoutsi, G., Bemporad, F., Calamai, M., Taddei, N., Dobson, C. M. & Chiti, F. (2005). Evidence for a mechanism of amyloid formation involving molecular reorganisation within native-like precursor aggregates. *J. Mol. Biol.* **351**, 910–922.
30. Ma, B. & Nussinov, R. (2002). Stabilities and conformations of Alzheimer's β-amyloid peptide oligomers ($A\beta_{16-22}$, $A\beta_{16-35}$, and $A\beta_{10-35}$): sequence effects. *Proc. Natl Acad. Sci. USA*, **99**, 14126–14131.
31. Gsponer, J., Haberthür, U. & Caflisch, A. (2003). The role of side-chain interactions in the early steps of aggregation: molecular dynamics simulations of an amyloid-forming peptide from the yeast prion Sup35. *Proc. Natl Acad. Sci. USA*, **100**, 5154–5159.
32. Klimov, D. & Thirumalai, D. (2003). Dissecting the assembly of $A\beta_{16-22}$ amyloid peptides into antiparallel β sheets. *Structure*, **11**, 295–307.
33. Wei, G., Mousseau, N. & Derreumaux, P. (2004). Sampling the self-assembly pathways of KFFE hexamers. *Biophys. J.* **87**, 3648–3656.
34. Hwang, W., Zhang, S., Kamm, R. D. & Karplus, M. (2004). Kinetic control of dimer structure formation in amyloid fibrillogenesis. *Proc. Natl Acad. Sci. USA*, **101**, 12916–12921.
35. Buchete, N.-V., Tycko, R. & Hummer, G. (2005). Molecular dynamics simulations of Alzheimer's beta-amyloid protofilaments. *J. Mol. Biol.* **353**, 804–821.
36. Lopez de la Paz, M., de Mori, G. M. S., Serrano, L. & Colombo, G. (2005). Sequence dependence of amyloid fibril formation: insights from molecular dynamics simulations. *J. Mol. Biol.* **349**, 583–596.
37. Pellarin, R. & Caflisch, A. (2006). Interpreting the aggregation kinetics of amyloid peptides. *J. Mol. Biol.* **360**, 882–892.
38. Kodali, R. & Wetzel, R. (2007). Polymorphism in the intermediates and products of amyloid assembly. *Curr. Opin. Struct. Biol.* **17**, 48–57.
39. Murphy, R. M. (2007). Kinetics of amyloid formation and membrane interaction with amyloidogenic proteins. *Biochim. Biophys. Acta*, **1768**, 1923–1934.
40. Rao, F. & Caflisch, A. (2004). The protein folding network. *J. Mol. Biol.* **342**, 299–306.
41. Caflisch, A. (2006). Network and graph analyses of folding free energy surfaces. *Curr. Opin. Struct. Biol.* **16**, 71–78.
42. Esler, W. P., Stimson, E. R., Jennings, J. M., Vinters, H. V., Ghilardi, J. R., Lee, J. P. *et al.* (2000). Alzheimer's disease amyloid propagation by a template-dependent dock-lock mechanism. *Biochemistry*, **39**, 6288–6295.
43. Gobbi, M., Colombo, L., Morbin, M., Mazzoleni, G., Accardo, E., Vanoni, M. *et al.* (2006). Gerstmann-Sträussler-Scheinker disease amyloid protein polymerizes according to the "dock-and-lock" model. *J. Biol. Chem.* **281**, 843–849.
44. Nguyen, P. H., Li, M. S., Stock, G., Straub, J. E. & Thirumalai, D. (2007). Monomer adds to preformed structured oligomers of abeta-peptides by a two-stage dock-lock mechanism. *Proc. Natl Acad. Sci. USA*, **104**, 111–116.
45. Jansen, R., Dzwolak, W. & Winter, R. (2005). Amyloidogenic self-assembly of insulin aggregates probed by high resolution atomic force microscopy. *Biophys. J.* **88**, 1344–1353.
46. Walsh, D., Hartley, D. M., Kusumoto, Y., Fezoui, Y., Condron, M., Lomakin, A. *et al.* (1999). Amyloid β-protein fibrillogenesis. structure and biological activity of protofibrillar intermediates. *J. Biol. Chem.* **274**, 25945–25952.
47. Fersht, A. (1999). *Structure and Mechanism in Protein Science.* W.H. Freeman and Company, New York, NY.
48. Tartaglia, G. G., Cavalli, A., Pellarin, R. & Caflisch, A. (2004). The role of aromaticity, exposed surface, and dipole moment in determining protein aggregation rates. *Protein Sci.* **13**, 1939–1941.